Active optical zoom for space-based imaging

David V. Wick[1a], Brett E. Bagwell[a], William C. Sweatt[a], Gary L. Peterson[b], Ty Martinez[c], Sergio R. Restaino[c], Jonathan R. Andrews[c], Christopher C. Wilcox[c], Don M. Payne[d], Robert Romeo[e]
[a]Sandia National Laboratories, PO Box 5800, MS 1188, Albuquerque, NM 87185-1188
[b]Breault Research Organization, 6400 E Grant Rd, Suite 350, Tucson, AZ 85715
[c]Naval Research Laboratory, c/oAFRL/DES, 3550 Aberdeen Ave SE, Kirtland AFB, NM 87117
[d]Narrascape, 737 Loma Vista Dr. NE, Albuquerque, NM 87106
[e]Composite Mirror Applications, Inc., 1638 S Research Loop, Suite 100, Tucson, AZ 85710

ABSTRACT

The development of sensors that are compact, lighter weight, and adaptive is critical for the success of future military initiatives. Space-based systems need the flexibility of a wide FOV for surveillance while simultaneously maintaining high-resolution for threat identification and tracking from a single, nonmechanical imaging system. In order to meet these stringent requirements, the military needs revolutionary alternatives to conventional imaging systems.

We will present recent progress in active optical (aka nonmechanical) zoom for space applications. Active optical zoom uses multiple active optics elements to change the magnification of the imaging system. In order to optically vary the magnification of an imaging system, continuous mechanical zoom systems require multiple optical elements and use fine mechanical motion to precisely adjust the separations between individual or groups of elements. By incorporating active elements into the optical design, we have designed, demonstrated, and patented imaging systems that are capable of variable optical magnification with no macroscopic moving parts.

Keywords: Active optics, Deformable mirrors, MEMS, Zoom lense**s**

1. INTRODUCTION

In order to achieve true optical magnification and overcome deficiencies in size, weight, and power requirements, we have previously proposed a revolutionary alternative to conventional mechanical zoom systems where moving lenses/mirrors and gimbals are replaced with active optics.[1-2] Active or adaptive optics,[3] such as liquid crystal (LC) spatial light modulators (SLMs) and deformable mirrors (DMs), have previously been proposed and demonstrated as variable focal-length elements.[4-6] Focus control is accomplished by systematically adjusting the optical path across the element to add/subtract quadratically varying phase. In fact, any aberration can be added or subtracted (focus is simply a low order aberration), providing a tremendous amount of flexibility.[7-9] By applying the appropriate voltage to each pixel or actuator, the optical path can be adjusted to create an optical wavefront that approximates the wavefront produced by a conventional lens or mirror. By changing those voltages appropriately, the "focal length" of the active element can be varied within the limits set by the dynamic range and the number of pixels or actuators.

By appropriately designing the optical system, these variable focal-length elements can provide the flexibility necessary to change the overall system focal length, and therefore magnification, that is normally accomplished with mechanical motion. The key to this concept is to create relatively large changes in system magnification with very small changes in the focal lengths of individual elements by leveraging the optical power of conventional optical elements surrounding the active optics. In addition to changing the focal length with a DM or SLM, optical tilt can also be added to the wavefront by appropriately adjusting the voltages. This allows magnification of ***any*** point within the FOV without physically moving some portion of the optical system. Thus, the object to be magnified does not have to lie on the optical axis as in a conventional system.

While our previous demonstrations have focused on small aperture systems, we are now looking at large aperture systems for telescopes. Utilizing this technique on meter class systems my improve capability without significantly

[1] dvwick@sandia.gov, ph. 505 844-2517

increasing size, weight, or power requirements. One approach is to utilize a deformable primary, coupled with an active tertiary mirror, to achieve active optical zoom from a large aperture telescope.

2. COMPOSITE MIRRORS

As size and weight are a premium for space-based applications, the development of light-weight, variable radius of curvature mirrors is an important component in a space-based active optical system. Composite Mirror Applications (CMA), working with the Naval Research Laboratory (NRL), is currently developing carbon fiber reinforced polymer (CFRP) mirrors for the Naval Prototype Optical Interferometer (NPOI). NPOI is the world's only long baseline optical interferometer operating in the visible region, i.e. wavelengths below 0.8 μm. It is also the only optical interferometer capable to recombine up to six beams, from different apertures, simultaneously.

Using carbon fiber construction for all components, including optics, CMA has delivered a 0.4 meter prototype telescope for testing, shown in Figure 1. CMA is currently fabricating a 1.4 meter telescope that will be less than 300 pounds. As all components of the telescope, including optics, are constructed from composite materials having a low coefficient of thermal expansion, dimensional changes due to temperature variations can be minimized. Also, since all optics are made from a single high precision tool, duplicate components can be manufactured for much less than traditional steel and glass telescopes.[10]

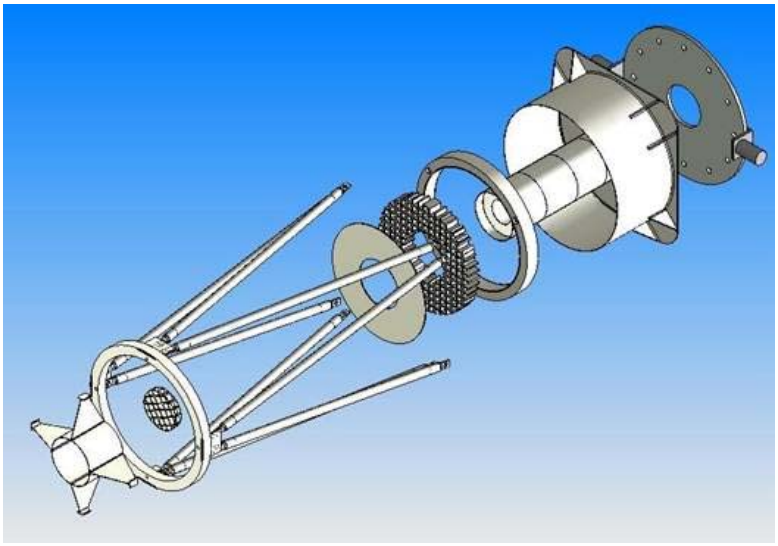

Figure 2: Exploded view of 0.4m CFRP telescope prototype

The optical telescope assembly (OTA), including all structural supports and optics, weighs roughly 10 Kg. As a comparison, a commercially available 0.4m Meade telescope weighs roughly 57 Kg. This lower mass and lower rotational inertia helps reduce the mount mass, and in turn, reduces the drive power requirements for tracking. The 0.4m system shown in figure 3 includes the drive motors, an electronics rack constructed from CFRP and aluminum, and a CFRP AO box and breadboard.

The performance of the drive system is dependent on 3 critical components: the drive motors and geometry, the encoders, and the servo electronics. A direct drive system was chosen for maximum stiffness and pointing precision. This drive system is realized with ultrasonic piezoelectric motors manufactured by Nanomotion, Ltd. driving a static ceramic ring. This unique drive configuration is possible because of the low mass (and low rotational inertia) of the system. Using the specifications provided by Nanomotion, the maximum slew speed is expected to exceed 20 deg/s with tracking speed exceeding 1 deg/sec.

The encoders are Renishaw optical encoders with a readout resolution of 0.04 arcseconds. The system accuracy is quoted as about 1 arcsecond which are largely systematic errors which can be compensated for in the mount drive model. The servo is controlled by a commercial control card designed for high accuracy and ease of implementation.

Figure 3- Lightweight telescope (in black) mounted on portable AO system (white) and lightweight mount (blue fork).

3. ACTIVE OPTICAL ZOOM

To show how a CFRP telescope could be used to achieve active optical zoom, we have investigated the first order design tradespace. If the system numerical aperture (f-number) is preserved, then the entrance pupil diameter increases when the system is zoomed, and is proportional to the zoom ratio. For example, suppose a system with an entrance pupil diameter of 1 *meter* and a field of view (half) of 0.5 *degrees*. If a 3:1 zoom ratio is desired, then the zoomed field of view is 0.167 *degrees* (one-third of 0.5 *degrees*), and the entrance pupil grows to a diameter of 3 *meters*.

The reason for this change is that the *Lagrange invariant* (or *optical invariant*, or *etendue*) must be preserved. For our purposes, the invariant (*H*) is

$$H = \frac{D}{2}\sin\theta = \frac{w}{2}(na), \qquad (1)$$

where D is the entrance pupil diameter, θ is the half field of view, w is the full width of the detector, and na is the numerical aperture. The numerical aperture is related approximately to the f-number by

$$f\# \approx \frac{1}{2(na)}. \qquad (2)$$

The size of the detector and the numerical aperture are fixed, so the value of *H* is the same in both the zoomed and unzoomed states. Inspection of the middle part of Equation (1) shows that decreasing the field of view θ requires a compensating increase in the entrance pupil diameter *D*.

To preserve the numerical aperture the second active mirror (the one closest to the detector) must be the aperture stop, or most be located at an image of the aperture stop. Figure (1) illustrates this with an active lens, rather than a mirror. In the figure the aperture stop is located beyond the active element. The top of the figure shows a backward trace of the marginal (blue) and chief (red) rays from the detector when the system in not zoomed. The marginal ray intersects the edge of the stop and the chief ray goes through the center of the stop. When the power of the active element is changed, as in the bottom half of Figure (1), the trajectory of the marginal and chief rays also changes. In effect, both the location and size of the aperture stop have changed, and this changes the system numerical aperture.

For a two-mirror system, closed form solutions for the mirror focal lengths and focal plane location appear below. Given the following quantities,

1. unzoomed entrance pupil diameter, D;

2. exit pupil diameter (secondary mirror diameter), d;

3. unzoomed field of view (half), θ;

4. image full width, w;

5. zoom ratio, R;

6. separation between the primary and secondary mirror, S;

we want to know the focal lengths, image plane location, and mirror deformations. The unzoomed system focal length, F, is given by

$$F = \frac{w}{2\tan\theta}. \quad (3)$$

Define a normalized separation, *s*, between the primary and secondary mirror,

$$s = \frac{S}{F}; \quad (4)$$

and the ratio *q* between the secondary and primary mirror diameters,

$$q = \frac{d}{D}. \quad (5)$$

The focal length of the primary is then given by

$$F_p = F\frac{Rs}{R-q}, \quad (6)$$

and the focal length of the secondary mirror is

$$F_s = F\frac{qs}{q+s-R}. \quad (7)$$

In both of these expressions, the value of R should be set to 1 to obtain the focal length in the unzoomed configuration. The distance from the secondary mirror to the image plane is

$$S_{2I} = F\frac{d}{D}. \quad (8)$$

The deformation of the primary mirror (stop on the secondary mirror) is given by

$$\Delta s_p = \frac{1}{16F}\left(D + w\frac{s}{q}\right)^2 \frac{q}{s}\frac{R-1}{R} \quad . \qquad (9)$$

The deformation in the secondary mirror is

$$\Delta s_s = -\frac{1}{16}\frac{d^2}{F}\frac{R-1}{qs} \quad . \qquad (10)$$

Figures (3) to (5) show the deformation (absolute value) of the primary and secondary mirrors as a function of separation between the mirrors at three fields of view. The unzoomed entrance pupil diameter is 333 *mm*. Three curves are shown in each graph. The solid red curve corresponds to a secondary mirror diameter of 50 *mm*. The dotted blue curve corresponds to a secondary mirror diameter of 100 *mm*. The dashed green curve corresponds to a secondary mirror diameter of 200 *mm*. Inspection of these figures shows that there is a trade between minimizing mirror deformation and minimizing system length. Small mirror deformations require a long system. Conversely, a short system requires large mirror deformations. Auxiliary optics between the active mirrors may be used to shorten the system.

One of the questions that arose from these calculations is: is it possible to reduce the amount of this deformation by placing reimaging optics or telescopes after the initial image plane? Alternatively, can we reduce the amount of deformation by using a fixed primary and secondary, and then reimaging the pupil and image with small active mirrors within the reimaging optics? The answer to both questions is *no*. If the numerical aperture and the aperture stop size and location are fixed, then there is a one-to-one relationship between the sag on the two active mirrors, regardless of where they are located (except that the second active mirror must be placed at an image of the aperture stop). An equation for the deformation on the first active mirror as a function of deformation on the second active mirror (located at an image of the aperture stop) is

$$\Delta s_2 = \frac{H(r-1)}{2r} + \frac{(4\Delta s_1)^2 + H^2(r-1)^2}{16\Delta s_1 r} \quad , \qquad (11)$$

where H is the Lagrange invariant and r is the zoom ratio. Note that this expression is independent of any optical design details. It depends only on the Lagrange invariant, which is the product of the entrance pupil diameter and half field of view, and the desired zoom ratio. Once these values are chosen, the required deformation in the mirrors is fixed. Auxiliary optics can reduce the length of the system, but cannot reduce the magnitude of the mirror deformations.

Figure (6) shows graphs of the amount of mirror deformation (from unzoomed to zoomed) for a zoom ratio of 3, an entrance pupil diameter of 333 *mm* (999 *mm* when zoomed), and three different unzoomed fields of view: 0.5, 0.1, and 0.05 *degrees*. Inspection of the graphs shows that there is minimum deformation for the first active mirror as a function of deformation in the second active mirror. For a field of view of 0.5 *degrees* and zoomed entrance pupil diameter of approximately 1 *meter*, the smallest possible deformation is 1 *mm*. The required deformation decreases with unzoomed field of view to a value of only 0.1 *mm* when the unzoomed field of view is 0.05 *degrees*. Because the field of view enters into Equation (11) only through the Lagrange invariant H, the same reduction in mirror deformation is obtained by holding the field of view fixed but reducing the entrance pupil diameter.

Primary Mirror

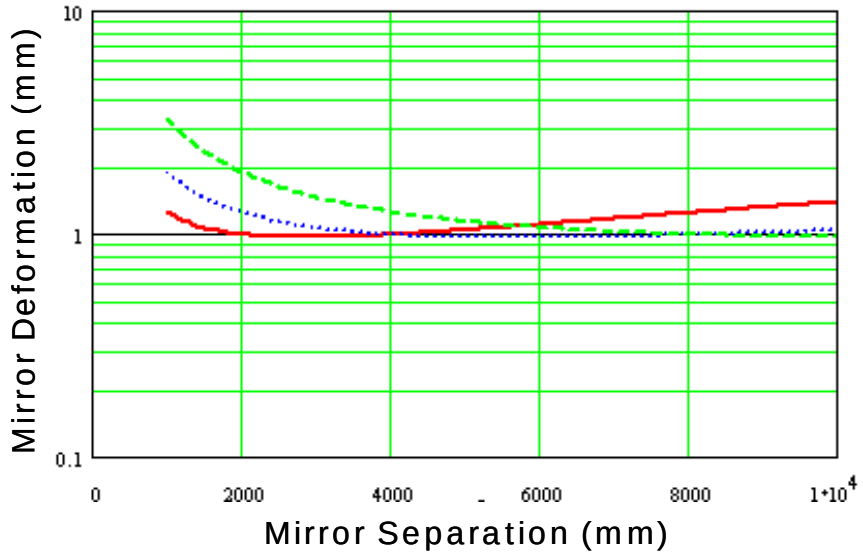

Secondary Mirror

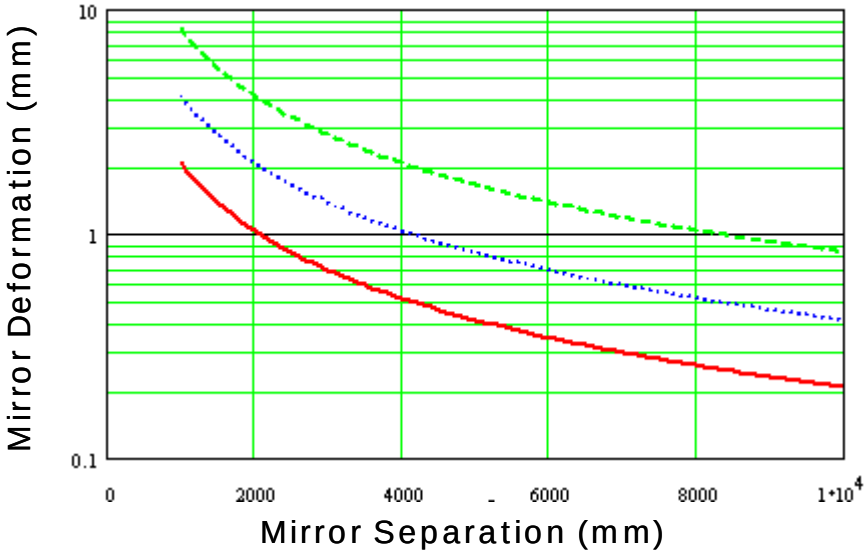

Figure (3): Mirror deformation as a function of mirror separation for three secondary mirror diameters: 50 *mm* (solid red curve), 100 *mm* (dotted blue curve), and 200 *mm* (dashed green curve). The half field of view is 0.5 *degrees.* The unzoomed primary mirror diameter is 333 *mm.*

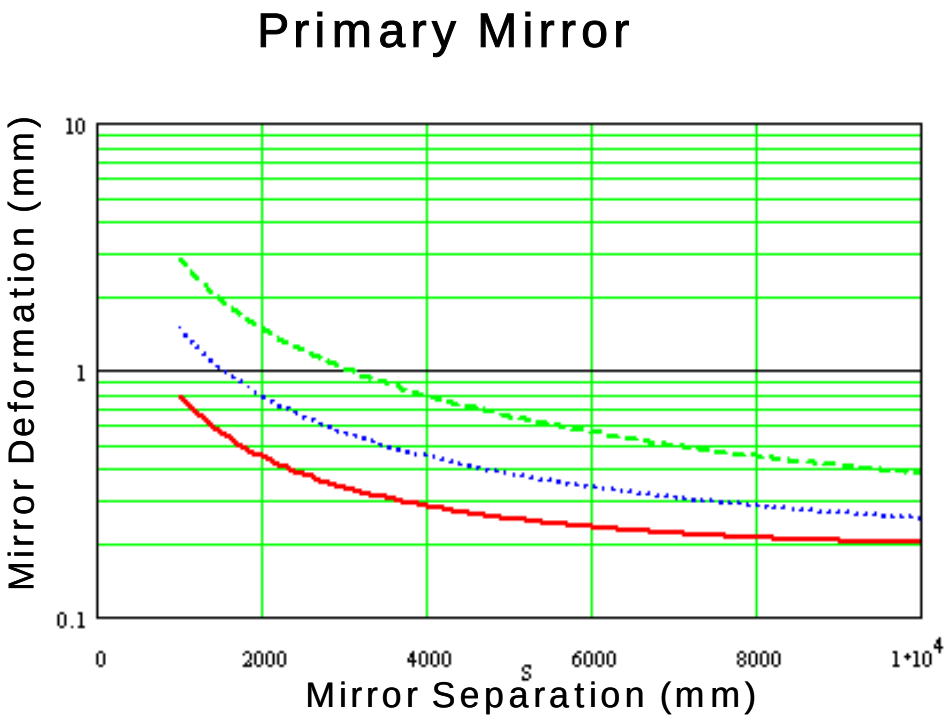

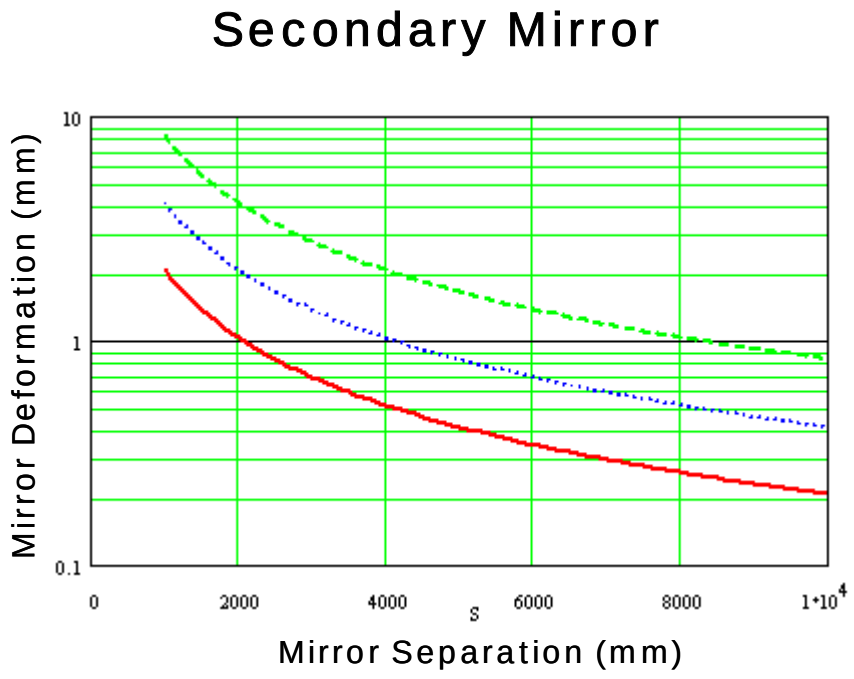

Figure (4): Mirror deformation as a function of mirror separation for three secondary mirror diameters: 50 *mm* (solid red curve), 100 *mm* (dotted blue curve), and 200 *mm* (dashed green curve). The half field of view is 0.1 *degrees*. The unzoomed primary mirror diameter is 333 *mm*.

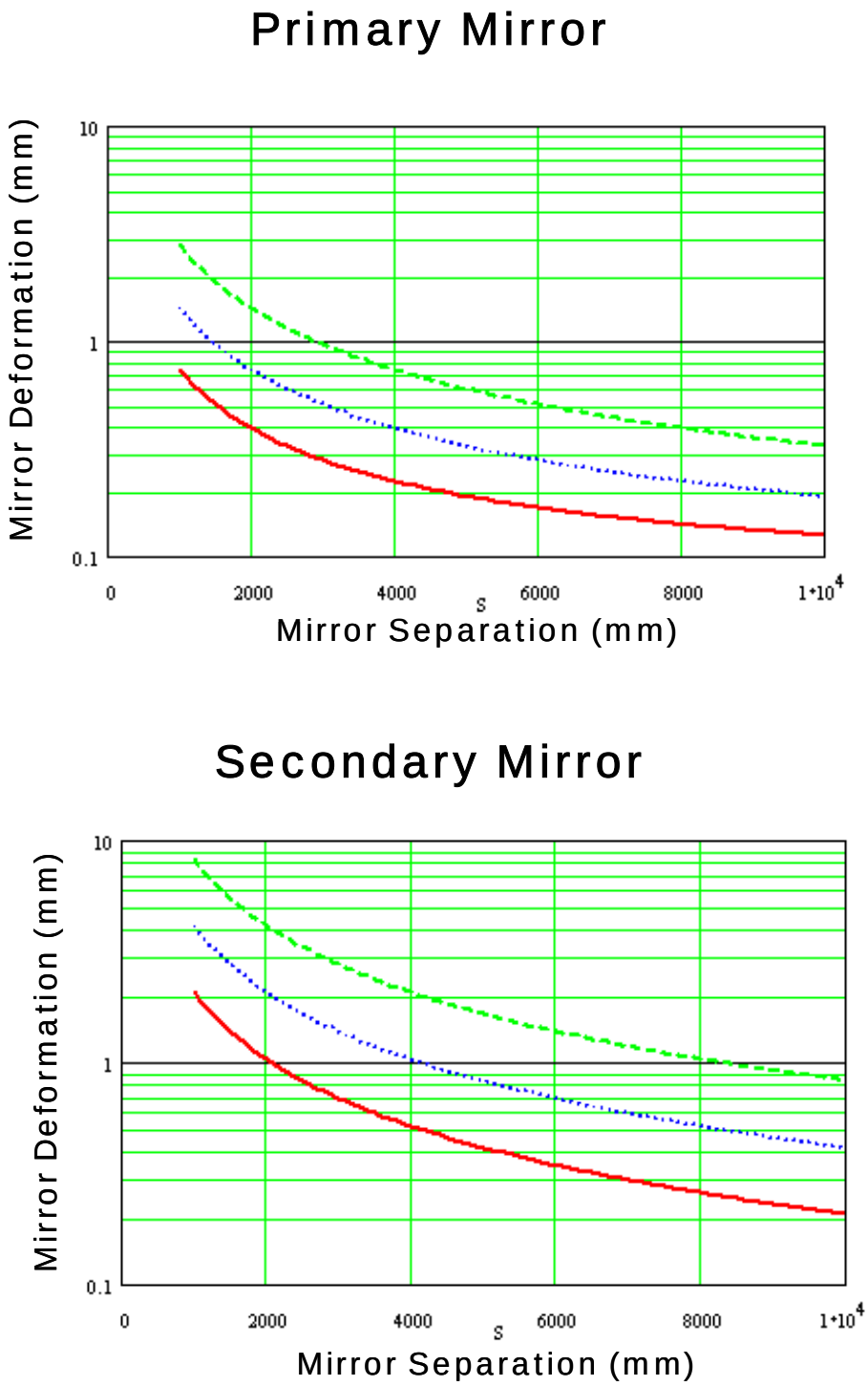

Figure (5): Mirror deformation as a function of mirror separation for three secondary mirror diameters: 50 *mm* (solid red curve), 100 *mm* (dotted blue curve), and 200 *mm* (dashed green curve). The half field of view is 0.05 *degrees*. The unzoomed primary mirror diameter is 333 *mm*.

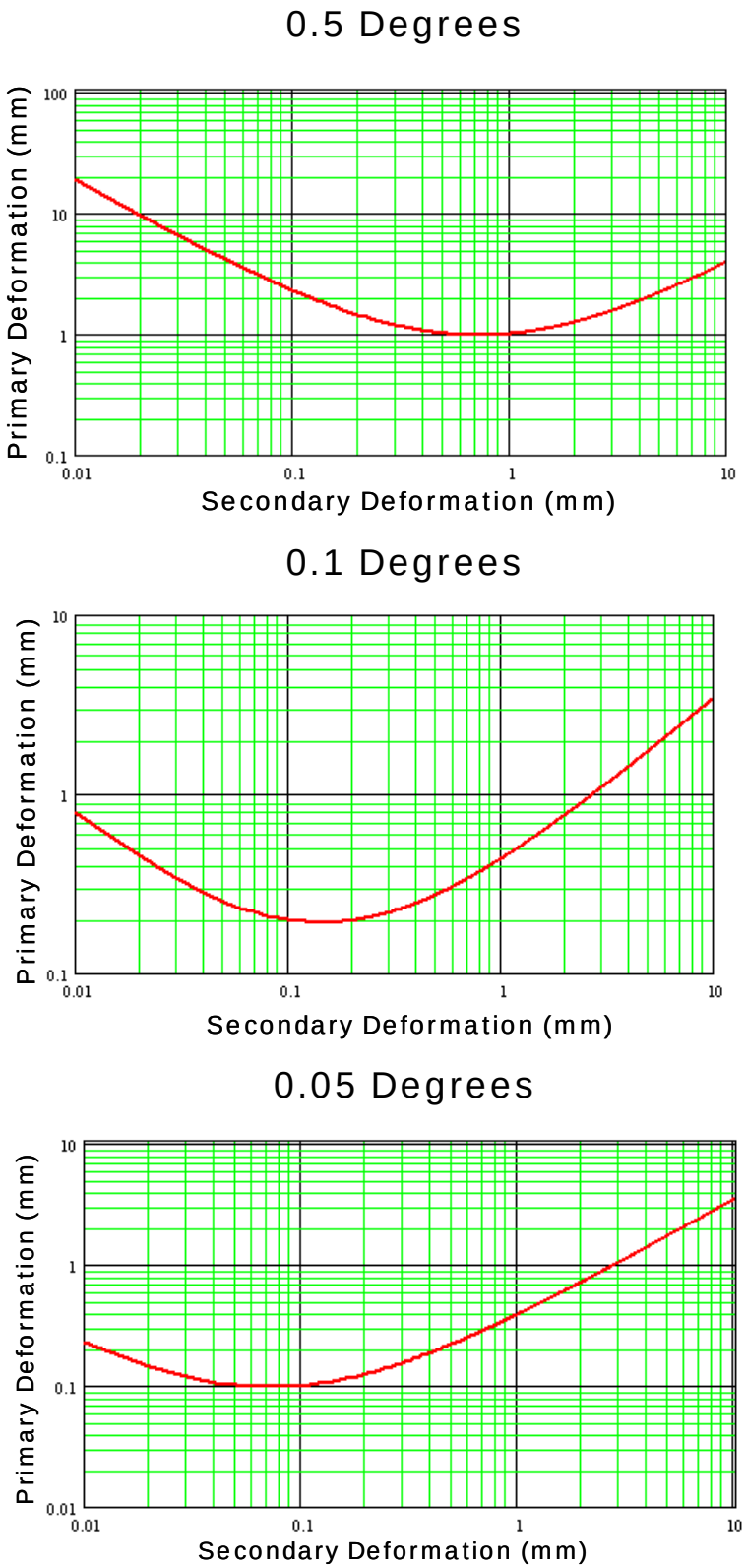

Figure (6): Primary mirror deformation as a function of secondary mirror deformation for an unzoomed entrance pupil diameter of 333 *mm* and zoom ratio of 3. Graphs are shown for a half field of view of 0.5, 0.1, and 0.05 *degrees*.

Applying these concepts, we have demonstrated off-axis magnification from a refractive imaging system using a custom built transmissive liquid crystal spatial light modulator from Boulder Nonlinear Systems, Inc. and a liquid crystal lens from Holochip, LLC. Preliminary images from that system are shown in Figure 7.

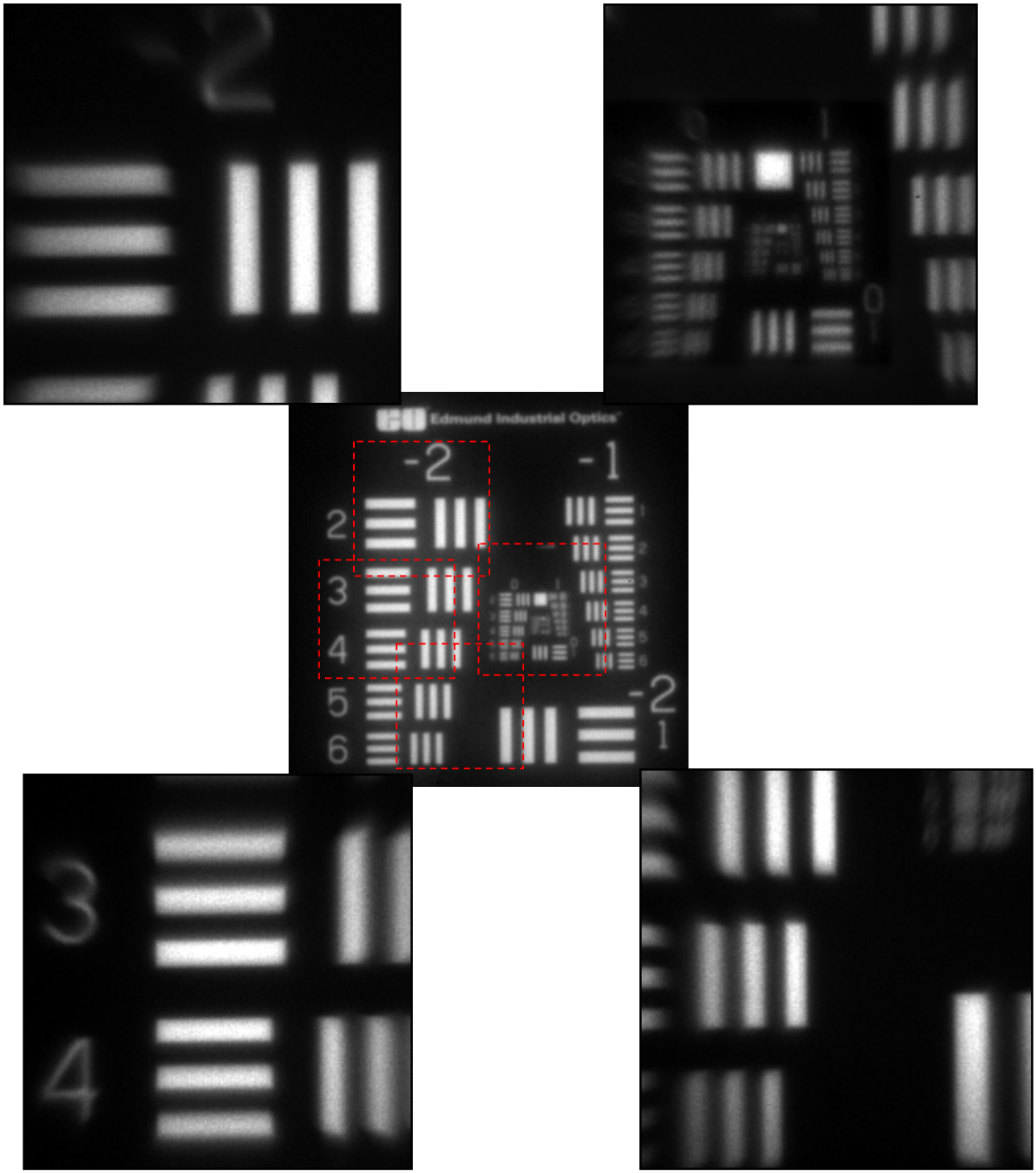

Figure 7: Off-axis magnification using two liquid crystal devices in a refractive, active optical zoom system.

4. CONCLUSIONS

Light weight, CFRP mirrors may be useful as large aperture, variable radius of curvature mirrors in an active optical system. A first order analysis of two-mirror active zoom systems shows that there is a fixed relation between the deformations of the two active mirrors. This relation is independent of system design details and depends only on the system Lagrange invariant and the zoom ratio. Auxiliary optics can reduce the overall length of a system, but cannot reduce the required deformation of the two mirrors. The second active mirror must be located at the aperture stop, or at an image of the aperture stop, to preserve the numerical aperture of the system. Under this condition, there is a minimum deformation on the first active mirror which cannot be altered by auxiliary optics. A fixed detector size and system numerical aperture (f-number) require that the entrance pupil increase in proportion to the zoom ratio. Closed form expressions for the focal length, location, and mirror deformation have been given for a two-mirror system.

REFERENCES

1. D.V. Wick and T. Martinez, “Adaptive optical zoom,” *Opt. Eng.,* **43**, 8-9 (2004).

2. T. Martinez, D.V. Wick, D.M. Payne, J.T. Baker, and S.R. Restaino, “Non-mechanical zoom system,” *Proceedings of the SPIE,* **5234**, 375-378 (2003).

3. R.K. Tyson, *Principles of Adaptive Optics, Second Edition,* Academic Press, San Diego (1998).

4. A. F. Naumov, G. Love, M. Y. Loktev, and F. L. Vladimirov, "Control optimization of spherical modal liquid crystal lenses ," *Opt. Express* **4**(9)**,** 344-352 (1999).

5. V. Laude, “Twisted-nematic liquid-crystal pixilated lens,” *Opt. Comm*. **153**, 134-152 (1998).

6. Y. Takaki and H. Ohzu, “ Liquid-crystal active lens: a reconfigurable lens employing a phase modulator,” *Opt. Comm*. **126**, 123-134 (1996).

7. D.V. Wick, T. Martinez, S.R. Restaino, and B.R. Stone, "Foveated imaging demonstration," *Opt. Express,* **10**, 60-65 (2002).

8. G. D. Love, “Wave-front correction and production of Zernike modes with a liquid-crystal spatial light modulator,” *Appl. Opt*. **36**, 1517-1524 (1997).

9. D. M. Pepper, C. J. Gaeta, and P. V. Mitchell, “Real-Time Holography, Innovative Adaptive Optics, and Compensated Optical Processors Using Spatial Light Modulators,” Chap. 14 in *Spatial Light Modulator Technology - Materials, Devices, and Applications,* U. Efron, ed., Marcel Dekker, Inc., New York (1995).

10. Andrews J.R., Penado F.E., Broome S.T., Wilcox C.C., Restaino S.R., Martinez T., Teare S.W., Santiago F. “Characterization of the lightweight telescope developed for the NPOI”, *Proc. SPIE Vol.* **6267,** (2006).